

Nonlinear magnetodynamic waves on magnetic materials

A. D. Boardman and M. M. Shabat

Applied Optics, Department of Physics, University of Salford, Salford M5 4WT, United Kingdom

R. F. Wallis

Department of Physics, University of California, Irvine, California 92717

(Received 1 March 1989; revised manuscript received 30 May 1989)

A study of nonlinear magnetodynamic waves on magnetic materials is presented. Attention is restricted to an exact theory of electromagnetic waves propagating along the single interface between a linear substrate consisting of a ferromagnetic and a strongly nonlinear magnetic cladding. It is assumed that the cladding consists of an artificial paramagnetic material and that only third-order nonlinearity is operating. It is shown that both TM and TE waves can propagate, with or without a linear limit. Nonreciprocity is found to be strong only in the cases that have linear limits, but the power dependence of this nonreciprocal behavior is quite dramatic and should lead to some applications. Many numerical examples are presented, supported by a detailed mathematical analysis.

I. INTRODUCTION

There is now a lot of interest in nonlinear waves in solid-state optics.¹⁻¹¹ In particular, nonmagnetic dielectric materials that exhibit optical hysteresis, arising from third-order nonlinearities, are expected to underpin the development of optical computing or signal processing. A search is therefore underway to find good nonlinear materials, and these will include artificial dielectrics, such as suspensions of polystyrene spheres for work at optical frequencies¹¹ and suspensions of short graphite fibers that will give strong Kerr-type nonlinear interactions, even at microwave frequencies.¹²

In the infrared frequency range, the inclusion of the magnetic properties of a material, through a *linear* permeability, can also influence optical bistability¹³ with hysteresis loops that are very small in area. This feature, is a function of the magnetic properties and illustrates the potential of magnetic materials for future devices. In the microwave frequency range, however, it is not only nonlinearity in the dielectric function¹² that is of interest. Nonlinearity may also appear as magnetic-field-dependent terms in the magnetic permeability.¹⁴ Although this kind of nonlinearity can arise at quite low power thresholds,^{14,15} in readily available insulator materials such as yttrium iron garnet (YIG), it is too weak to change the modal fields of thin-film guided waves. In order to achieve this, strongly nonlinear magnetic materials will need to become available. If experience with nonmagnetic dielectric materials is to be relied upon, then the search for large intrinsic nonlinearities will not be easy but exploiting suitable waveguiding formats¹⁻⁸ and the use of artificial¹⁶ nonlinear magnetic media hold out considerable promise. Such materials can be created¹⁶ with a suspension of magnetic spheres in a suitable medium such as a liquid. Nd spheres in water has been suggested, for example.¹⁶ It has been estimated that paramagnetic or diamagnetic spheres¹⁶ of radius 2×10^{-6}

m, with a density 10^{16} m^{-3} , dispersed in diamagnetic liquid will display a large nonlinearity at reasonable microwave powers. Unlike the artificial dielectric systems,^{11,12} such magnetic suspensions remain to be investigated experimentally but will prove to be very interesting.

In the optical case it has been argued that liquid suspensions of nonmagnetic spheres in a standing electromagnetic wave field experience a force that moves the spheres into high-field regions of the standing wave pattern. This induced movement of particles raises the average refractive of the medium in the high-field regions of the artificial dielectric so that the whole suspension mimics a conventional nonlinear medium with a high, positive, or negative, Kerr coefficient.¹¹ This same idea has also been proposed for aerosols of glass spheres¹⁷ subjected to electrostrictive modulation of their density. The fact that such artificial nonlinear media have nonlinear coefficients that are a factor of 10^5 higher than those of other readily available nonlinear, nonmagnetic, materials¹¹ encourages the belief that artificial nonlinear magnetic suspensions of magnetic spheres will behave in the same manner. It should be emphasized, at this stage, however, that the appropriate parameters must be estimated, but the rather large artificial nonlinear coefficients are at least expected to be proportional to the radius of the spheres.¹⁶

Over the last two decades a lot of work in solid-state physics has been devoted to surface polaritons.¹⁸ This has mainly been based upon an optical point of view and has largely centered upon nonmagnetic dielectrics. A small amount of work does exist on surface magnon polaritons in which surface waves at the interface between two semi-infinite magnetic materials or on a thin ferromagnetic film have been considered.^{19,20} This polariton regime is sufficiently close to the light line for retardation effects to have to be taken into account. For this reason, and because a distinction must be drawn between this and magnetostatic waves, it has also been referred to as the magnetodynamic regime.²¹⁻²³ The waves are *non-*

reciprocal if they propagate perpendicularly to an applied magnetic field lying in the surface. *Nonreciprocity* means the dispersion relation is not the same in the positive and negative wave number directions.

The purpose of this paper is to examine the behavior of surface nonlinear magnetodynamic (polariton) waves that are propagating along the interface between a semi-infinite, weakly nonlinear substrate and the kind of dominant strongly nonlinear magnetic, semi-infinite, cladding that was defined earlier. The strong nonlinearity of a magnetic cladding medium will always be assumed to dominate that of a magnetic substrate, if it is associated with a wave traveling along the interface. This assumption allows us to completely *neglect* the weak, intrinsic, nonlinearity attainable in the YIG substrate. Self focusing, in frequency ranges for which no linear eigenvalue exists¹⁻⁸ is anticipated, and only third-order nonlinearity is considered on the grounds that all harmonic generation can be ignored because of lack of phase matching. In frequency bands for which linear eigenvalues exist, harmonic generation in any case corresponds to very weak, driven, harmonic waves lying outside the linear eigenfrequency band. It should be mentioned that although the mathematical infrastructure of the application reported here is unique, there will be a similarity of attack between the methods employed and some previous work on nonmagnetic materials.^{1,3,5} This is also true of many linear problems, however.

II. THEORY OF TM WAVES

The guiding structure to be considered consists of a linear semi-infinite ferri(ferro)magnetic insulator substrate assumed from now on to be YIG, and a semi-infinite nonlinear magnetic cladding in contact everywhere on the $z=0$, plane as shown in Fig. 1. It must be emphasized that the substrate will always be assumed to be *linear*, compared to the cladding, and that it exists in frequency windows that make it appear to be ferromagnetic.

It is well known that there is no linear band for TM surface waves¹⁹ propagating along the x axis, but experience with the nonmagnetic dielectric case^{1,4,7} shows that

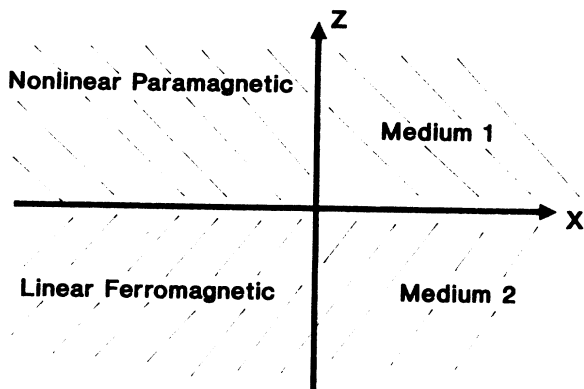


FIG. 1. Coordinate system for the single interface between a nonlinear paramagnetic cladding and a linear ferromagnetic cladding.

there ought to be *nonlinear* TM waves above a certain power threshold. Since the latter has to be reached before these are possible, they may require very high powers, possibly beyond the current experimental reach, to drive them. It is to these nonlinear waves that this section is addressed.

The TM waves carry the magnetic field \mathbf{H} and electric field \mathbf{E} components

$$\mathbf{H} = [0, H_y(z), 0] e^{i(kx - \omega t)}, \quad (1)$$

$$\mathbf{E} = [E_x(z), 0, E_z(z)] e^{i(kx - \omega t)}, \quad (2)$$

where ω is the angular frequency and k is the wave number. For this polarization the YIG substrate can only affect the propagation through a frequency independent permeability $\mu_2 = \mu_B$. The off-diagonal terms of the usual Polder tensor are brought into action by TE waves, that are to be considered later on. Some comments on the parameters normally assumed for YIG are now appropriate.²¹⁻²⁴ μ_B is interpreted as the background permeability caused by other magnetic dipole excitations,¹⁹ such as optical magnons. It is interesting that, because μ_B is close to unity, it is usually taken as unity in practical device designs²¹⁻²³ without apparent penalty. $\mu_B \approx 1.25$ in practical frequency ranges for YIG, however, and the background dielectric constant is also not equal to unity. It is sometimes assumed to be so,^{19,20} but it has appeared in the literature with quite a wide range of values.¹⁹⁻²⁴ Both μ_B and the background dielectric constant can lead to branches in the dispersion relationship that exist because of their deviation from unity.¹⁹⁻²³

In the presence of the microwave field associated with a TM wave propagating along the interface, the nonlinear permeability of an isotropic magnetic cladding is given by¹⁶

$$\mu^{\text{NL}} = \mu_L + \alpha H_y^2. \quad (3)$$

This expression arises because from an expansion of the permeability about an applied static field H_0 , and terms that could lead to harmonic generation are neglected.

Hence H_y is now the ac magnetic field carried out by the TM wave. $\mu_1 = \mu_L$ is the linear part of the permeability and α is a nonlinear coefficient. H_y is also real because only stationary, nonradiating waves will be considered.^{3,5}

Maxwell's curl equations for the nonlinear medium have the simple form

$$\text{curl} \mathbf{E} = i\omega\mu_0\mu^{\text{NL}}\mathbf{H}, \quad (4)$$

$$\text{curl} \mathbf{H} = -i\omega\epsilon_0\epsilon_1\mathbf{E}, \quad (5)$$

where ϵ_1 is the relative dielectric constant of the nonlinear medium. Equations (3) and (4) yield

$$ikE_z - \frac{\partial}{\partial z} E_x = -i\omega\mu_0\mu^{\text{NL}}H_y, \quad (6)$$

$$\frac{\partial}{\partial z} H_y = i\omega\epsilon_0\epsilon_1 E_x, \quad (7a)$$

$$kH_y = -\omega\epsilon_0\epsilon_1 E_z. \quad (7b)$$

Hence,

$$\frac{\partial^2}{\partial z^2} H_y - (k_1^2 - k_0^2 \epsilon_1 \alpha H_y^2) H_y = 0, \quad (8)$$

where $k_0^2 = \omega^2/c^2 = \epsilon_0 \mu_0 \omega^2$. ϵ_0 and μ_0 are the dielectric permittivity and magnetic permeability of free space, respectively, and

$$k_1^2 = k^2 - k_0^2 \epsilon_1 \mu_L. \quad (9)$$

Equation (8) is a nonlinear differential equation that can be solved exactly,¹⁻⁸ and the first integral obtained by multiplying through by $\partial H_y / \partial z$ and integrating over z , is

$$\left[\frac{\partial H_y}{\partial z} \right]^2 - (k_1^2 - \frac{1}{2} k_0^2 \epsilon_1 \alpha H_y^2) H_y^2 = C, \quad (10)$$

where C is a constant of integration. For the surface waves under investigation here $H_y \rightarrow 0$ and $\partial H_y / \partial z \rightarrow 0$, as $z \rightarrow \infty$ so that $C = 0$. This conclusion also implies that there is no radiation leaving the surface or returning to it.

The solution to equations of the form assumed by Eq. (10) has the form now well known for TE nonlinear waves propagating along the boundary between two nonmagnetic dielectric media [see, for example, Eq. (1) in Ref. 5 and Eq. (24) in Ref. 4]. It is

$$H_y(z) = \frac{1}{k_0} \left[\frac{2}{\alpha \epsilon_1} \right]^{1/2} \frac{k_1}{\cosh[k_1(z - z_0)]}, \quad (11)$$

where z_0 is a constant of integration that defines the position of a self-focused peak in H_y .

In a linear ferri(ferro)magnet the field corresponding to a surface wave at $z = 0$ is given by

$$H_y(z) = H_L e^{+k_2 z}, \quad (12)$$

where H_L is the amplitude of H_y at $z = 0$ and $k_2^2 = k^2 - k_0^2 \epsilon_2 \mu_2$. The usual electromagnetic boundary conditions that express the continuity of the tangential components of \mathbf{E} and \mathbf{H} and the normal component of the electric displacement \mathbf{D} at the boundary $z = 0$ now apply. In particular, the continuity of the tangential component of \mathbf{H} yields

$$H_L = \frac{k_1}{k_0} \left[\frac{2}{\alpha \epsilon_1} \right]^{1/2} \frac{1}{\cosh(k_1 z_0)}. \quad (13)$$

The continuity condition of the tangential component of \mathbf{E} gives

$$\frac{k_1^2}{k_0 \epsilon_1} \left[\frac{2}{\alpha \epsilon_1} \right]^{1/2} \frac{\sinh(k_1 z_0)}{\cosh^2(k_1 z_0)} = \frac{k_2}{\epsilon_2} H_L. \quad (14)$$

The elimination of H_L from Eqs. (13) and (14) gives a dispersion relation for the nonlinear TM surface waves in the form

$$\tanh(k_1 z_0) = \frac{k_2 \epsilon_1}{k_1 \epsilon_2}. \quad (15)$$

This dispersion relation can now be used to obtain bounds on the range of allowed values of the wave vector k . Since we assume that the dielectric constants ϵ_1 and ϵ_2

are positive, and since the decay constants k_1 and k_2 must also be positive for a surface wave, the right-hand side of Eq. (15) is positive. The positive values of the hyperbolic tangent on the left-hand side, therefore, lie in the range from zero to unity, so we must have

$$k^2 < \frac{k_0^2 \epsilon_1 \epsilon_2 (\epsilon_1 \mu_2 - \epsilon_2 \mu_L)}{\epsilon_1^2 - \epsilon_2^2}, \quad (16)$$

which defines an upper cutoff on the value of the wave vector k that approaches infinity as $\epsilon_1 \rightarrow \epsilon_2$. Actually, as $z_0 \rightarrow \infty$, $\tanh(k_1 z_0) \rightarrow 1$ so that the cutoff is associated with the self-focused peak in the field moving out to infinity. It will be shown later that this cutoff leads to a corresponding cutoff on the power flow. The requirements that $k_1^2 > 0$ and $k_2^2 > 0$ for a surface wave together give the relations

$$k^2 > k_0^2 \epsilon_1 \mu_L, \quad (17)$$

$$k^2 > k_0^2 \epsilon_2 \mu_2,$$

so that there is a lower cutoff on k as well. We must also note from Eq. (16) that, if $\epsilon_1 > \epsilon_2$, we must have $\epsilon_1 \mu_2 > \epsilon_2 \mu_L$.

Yet another inequality can be obtained by eliminating z_0 from the boundary conditions, Eqs. (13) and (14), to yield the result

$$k^2 = \frac{k_0^2 \epsilon_1 \epsilon_2}{\epsilon_1^2 - \epsilon_2^2} (\epsilon_1 \mu_2 - \epsilon_2 \mu_L - \frac{1}{2} \epsilon_2 \alpha H_L^2). \quad (18)$$

Again taking $\epsilon_1 > \epsilon_2$ and noting that k^2 must be positive, we obtain the inequalities

$$\frac{1}{2} \epsilon_2 \alpha H_L^2 < \epsilon_1 \mu_2 - \epsilon_2 \mu_L, \quad (19)$$

$$\epsilon_2 \mu_2 - \epsilon_1 \mu_L > \frac{1}{2} \epsilon_1 \alpha H_L^2. \quad (20)$$

Thus, depending on the material parameters, there is a maximum value of the magnetic field amplitude H_L .

The power flow in the direction of propagation (x direction) is given by

$$P = \frac{1}{2} \int (\mathbf{E} \times \mathbf{H}^*)_x dz = -\frac{1}{2} \int E_z H_y^* dz. \quad (21)$$

Hence P^{NL} , the power flow in the nonlinear medium, is

$$\begin{aligned} P^{\text{NL}} &= \frac{k k_1^2}{\alpha \omega k_0^2 \epsilon_0 \epsilon_1^2} \int_0^\infty \frac{dz}{\cosh^2[k_1(z - z_0)]} \\ &= \frac{k k_1^2}{\alpha \omega k_0^2 \epsilon_0 \epsilon_1^2} \int_{-z_0}^\infty \frac{dz'}{\cosh^2(k_1 z')}, \end{aligned} \quad (22)$$

where $z' = z - z_0$. The quantity z_0 is the position of maximum power density and when it moves to infinity, the power flow reaches the value

$$P^{\text{NL}} = \frac{k k_1^2}{\alpha \omega k_0^2 \epsilon_0 \epsilon_1^2} \int_{-\infty}^\infty \frac{dz'}{\cosh^2(k_1 z')} = \frac{k k_1}{\alpha \omega k_0^2 \epsilon_0 \epsilon_1^2}. \quad (23)$$

The substituting of the maximum value of k , as specified by Eq. (16) then, gives the following cutoff power flow:

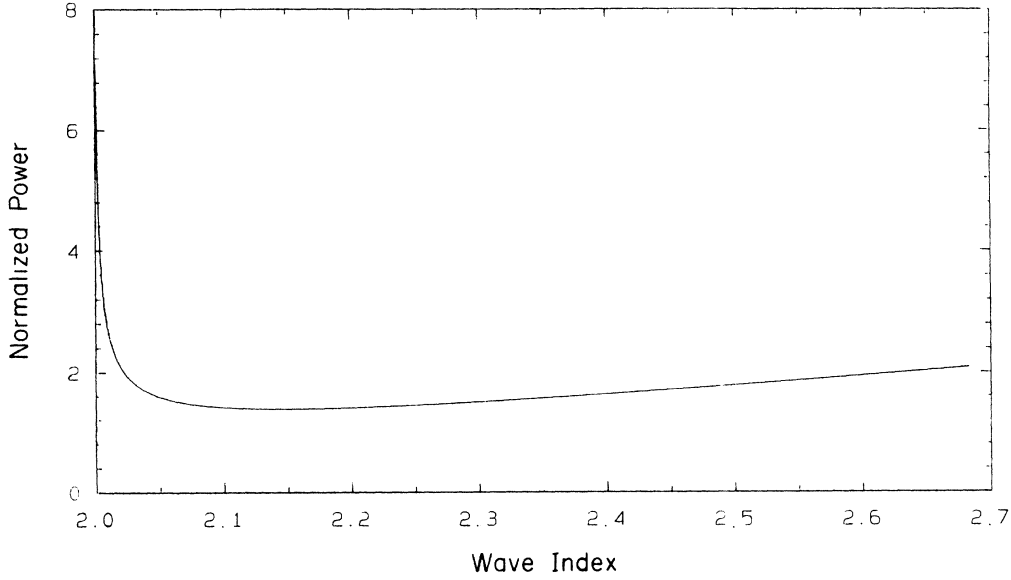


FIG. 2. TM waves: normalized power flow along the x direction as a function of wave index ($n = ck/\omega$, $\mu_1 = \mu_L = 1.29$, $\epsilon_1 = \epsilon_L = 2.3$, $\mu_2 = 2$, $\epsilon_2 = 2$). Frequency $f = 90$ GHz. $\alpha = 8.869 \times 10^{-8} \text{ m}^2 \text{ A}^{-2}$. The normalized power is P/P_0 , where $P_0 = 1/(2\omega\alpha\epsilon_0)$. $\epsilon_0 = 8.85 \times 10^{-12} \text{ F m}^{-1}$ is the permittivity of free space.

$$P_c^{\text{NL}} = \frac{2k_1}{\alpha\omega k_0 \epsilon_0 \epsilon_1^2} \left[\frac{\epsilon_1 \epsilon_2 (\epsilon_1 \mu_2 - \epsilon_2 \mu_1)}{\epsilon_1^2 - \epsilon_2^2} \right]^{1/2}. \quad (24)$$

P^L , the power flow in the linear medium, is given by

$$P^L = \frac{k}{4\omega\epsilon_0\epsilon_2 k_2} H_L^2, \quad (25)$$

$$P^L = \frac{kk_1^2}{2\alpha\omega k_0^2 \epsilon_0 \epsilon_1 \epsilon_2 k_2 \cosh^2(k_1 z_0)},$$

from which it can be seen that when $z_0 \rightarrow \infty$, $P^L \rightarrow 0$, and all of the power flow is in the nonlinear medium.

III. NUMERICAL RESULTS FOR TM WAVES

The dispersion equation, in this case, coincides with the dependence of the total power flow in the x direction upon the surface-guided wave index $n = ck/\omega$. The interface, in its linear state, will not support TM surface waves so it is not unexpected¹⁻⁷ that a power threshold has to be exceeded before nonlinear waves can propagate. This is shown in Fig. 2, together with two other features. First, the power approaches an infinite value as the wave

index becomes smaller on the left of the minimum. Equation (17) shows that this lower limit $n_{\min} = (\mu_2 \epsilon_2)^{1/2} = 2$, for the data chosen. Data required to illustrate this work are not easy to find, so parameter values have been selected that have been referred to in the literature at least as possibilities.^{16,19-26} These are shown in Table I. As $(\mu_2 \epsilon_2)^{1/2}$ is approached most of the power resides in the linear medium, necessitating very large powers to drive the nonlinear wave. Note that the power in Fig. 2 is normalized with

$$P_0 = \frac{1}{2\alpha\omega\epsilon_0} = 1.127 \text{ MW m}^{-1}.$$

This is quite high but the power essentially scales as the inverse of $\omega\alpha$ so that working at low frequencies requires large α to offset this fact. As n increases, the power passes through a minimum and finally reaches

$$n_{\max} = n_{\min} \left[\epsilon_1 \left[\epsilon_1 - \frac{\epsilon_2 \mu_1}{\mu_2} \right] / (\epsilon_1^2 - \epsilon_2^2) \right]^{1/2} = 2.68,$$

the upper wave-number limit given by Eq. (16) and finite power limit given by Eq. (24). At this extinction point

TABLE I. Parameter values (obtained from indicated references) used in figures.

		Nonlinear cladding			
α ($\text{m}^2 \text{ A}^{-2}$)	μ_1 ($=\mu_1$)	ϵ_1	Figure number	Reference	
8.869×10^{-8}	1.29	2.3	2, 3, 4, 5	25, 16	
		Linear substrate			
$\mu_0 H_0$ (G)	$\mu_0 M_0$ (G)	μ_2 ($=\mu_\beta$)	ϵ_2	Figure number	Reference
		2	2	2	24, 26
500	1000	1.25	1	7	19
500	1750	1	16	8-13	21-23

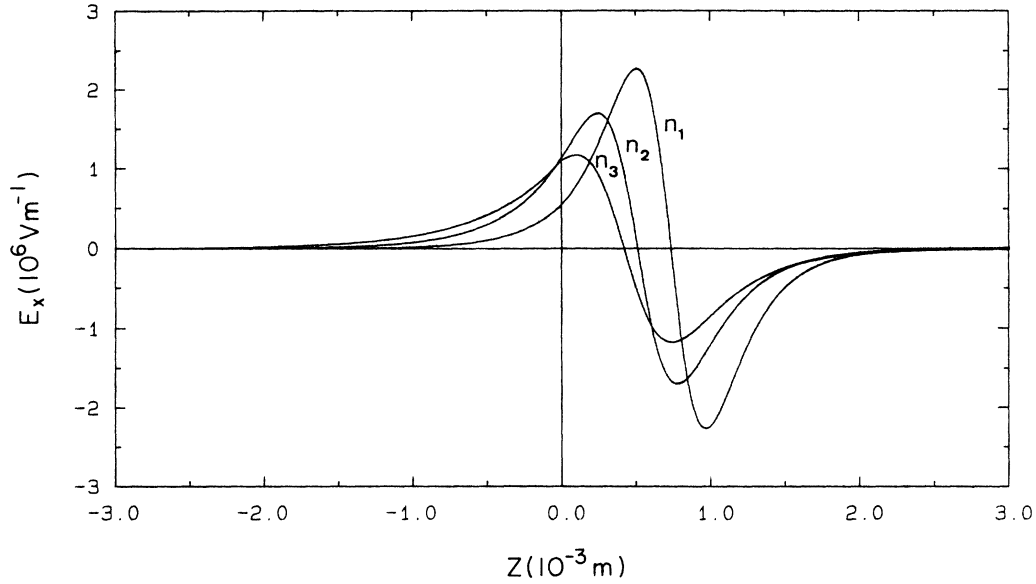


FIG. 3. TM waves: Variation of the E_x field component across the interface for the wave index values $n_1=2.645$, $n_2=2.449$, $n_3=2.36$. These refer to curves with descending maximum values. $f=90$ GHz. $\alpha=8.869 \times 10^{-8} \text{ m}^2 \text{ A}^{-2}$. Data from Fig. 2.

any self-focused peak has moved out to infinity and all the power flow is in the nonlinear medium. Figures 3–5 show, respectively, the shape of the nonlinear E_x , E_z , and H_y electromagnetic field components in the vicinity of the interface for the n values $\sqrt{5}$, $\sqrt{6}$, and $\sqrt{7}$ conveniently chosen to represent typical values in the permitted range $2 < n < 2.68$.

IV. THEORY OF TE WAVES

In this case the permeability tensor of the linear magnetic substrate medium, for this geometry, is

$$\boldsymbol{\mu}(\omega) = \begin{pmatrix} \mu_{xx} & 0 & \mu_{xz} \\ 0 & \mu_2 & 0 \\ -\mu_{xz} & 0 & \mu_{xx} \end{pmatrix}, \quad (26)$$

where the magnetization and the external magnetic field are in the y direction and

$$\mu_{xx} = \mu_B \left[\frac{\omega_0(\omega_0 + \omega_m) - \omega^2}{\omega_0^2 - \omega^2} \right],$$

$$\mu_{xz} = i\mu_B \frac{\omega\omega_m}{\omega_0^2 - \omega^2}, \quad \mu_2 = \mu_B$$

are the usual Polder tensor elements, with $\omega_0 = \gamma\mu_0 H_0$ and $\omega_m = \gamma\mu_0 M_0$. H_0 is the applied magnetic field, $\gamma = 1.76 \times 10^{11} \text{ s}^{-1} \text{ T}^{-1}$ is the gyromagnetic ratio, and M_0 is the dc saturation magnetization.

The electric and magnetic field vectors of the electromagnetic field for the TE waves take the form

$$\mathbf{E} = [0, E_y(z), 0] e^{i(kx - \omega t)}, \quad (27)$$

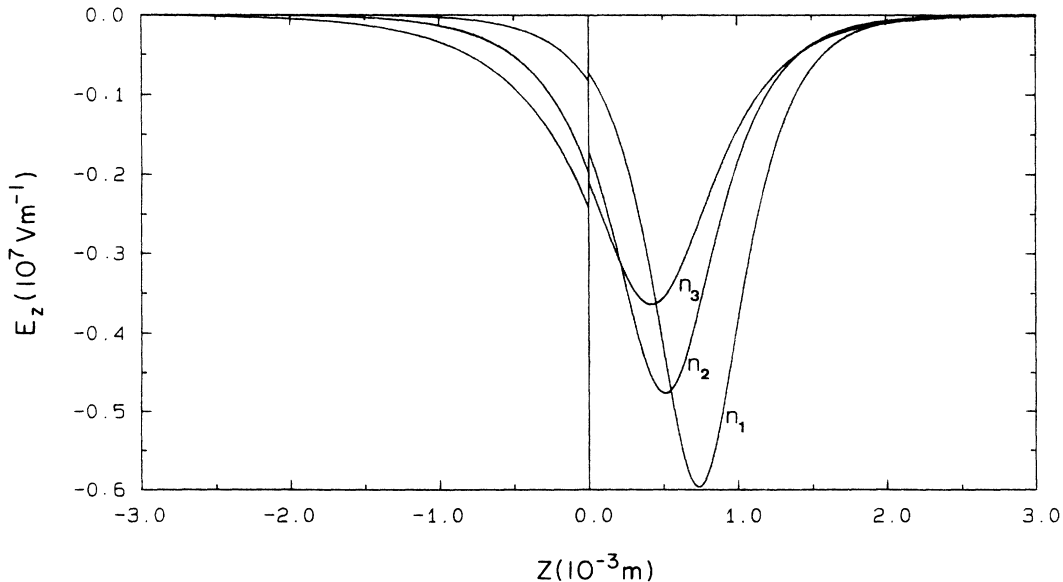


FIG. 4. TM waves: Variation of the E_z field component across the interface for the data of Fig. 3.

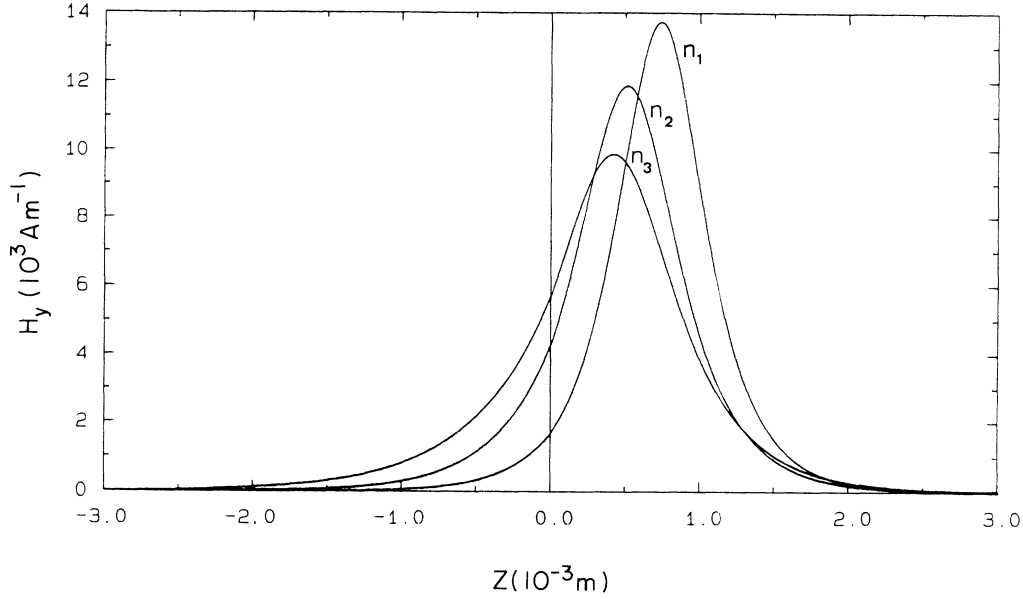


FIG. 5. TM waves: Variation of the H_y field component across the interface for the data of Fig. 3.

$$\mathbf{H} = [H_x(z), 0, H_z(z)] e^{i(kx - \omega t)}, \quad (28)$$

and the relevant components of Maxwell's equations for the nonlinear medium are

$$\frac{\partial E_y}{\partial z} = -i\omega\mu_0\mu^{\text{NL}}H_x, \quad (29a)$$

$$kE_y = \omega\mu_0\mu^{\text{NL}}H_z, \quad (29b)$$

$$\frac{\partial H_x}{\partial z} - ikH_z = -i\omega\epsilon_0\epsilon_1E_y. \quad (30)$$

In order to make contact with previous analogous work on nonlinear TM waves,^{3,5} we eliminate E_y rather than H_x and H_z from Eqs. (29), and exploit the $\pi/2$ phase difference between H_x and H_z for TE waves with definitions $H_x = h_x$, $H_z = ih_z$ to obtain

$$\frac{\partial^2 h_x}{\partial z^2} + k \frac{\partial h_z}{\partial z} = -k_0^2 \epsilon_1 \mu^{\text{NL}} h_x, \quad (31)$$

$$\frac{\partial h_x}{\partial z} = -\frac{1}{k} (k^2 - k_0^2 \epsilon_1 \mu^{\text{NL}}) h_z. \quad (32)$$

The first integral is obtained from Eq. (31) by multiplying it by $\partial h_x / \partial z$ and utilizing Eq. (32) to give

$$\frac{\partial}{\partial z} \left[\frac{\partial h_x}{\partial z} \right]^2 - k^2 \frac{\partial h_z^2}{\partial z} + k_0^2 \epsilon_1 \mu_L \frac{\partial h^2}{\partial z} + \frac{1}{2} k_0^2 \epsilon_1 \alpha \frac{\partial h^4}{\partial z} = 0, \quad (33)$$

where $h^2 = h_x^2 + h_z^2$. The integral of Eq. (33) with respect to z gives

$$[2n^2 - \epsilon_1(\mu_L + \alpha h^2)]h_z^2 - n^2 h^2 + \frac{\alpha n^2 h^4}{2(\mu_L + \alpha h^2)} = 0, \quad (34)$$

where the constant of integration is zero, since then the

magnetic field components (h_x, h_z) describe a surface wave localized at the interface $z=0$ and $n^2 = k^2/k_0^2$.

If we regard the nonlinear parameter α as small, we can obtain an approximate expression for the first integral correct to first order in α that has the form

$$(2n^2 - \epsilon_1 \mu_L) h_z^2 - n^2 h^2 + \frac{\alpha h^2}{2\mu_L} (n^2 h^2 - 2\epsilon_1 \mu_L h_z^2) = 0. \quad (35)$$

In the linear medium, the differential equation satisfied by E_y is

$$\frac{\partial^2 E_y}{\partial z^2} - \gamma_2^2 E_y = 0, \quad (36)$$

where

$$\mu_V = \mu_{xx} + \frac{\mu_{xz}^2}{\mu_{xx}}, \quad \gamma_2^2 = k^2 - k_0^2 \mu_V.$$

The solution of Eq. (36) corresponding to a surface wave localized at $z=0$, is given by

$$E_y(z) = E_L e^{-\gamma_2 z}. \quad (37)$$

Once again the $\pi/2$ phase relation between the field components, permits the definitions

$$H_x = h_x, \quad H_z = ih_z, \quad E_y = ie_y.$$

So that the field components h_x and h_z , in terms of e_y , are

$$h_x = \left[\frac{-\gamma_2 \mu_{xx} - ik \mu_{xz}}{\omega \mu_0 \mu_{xx} \mu_V} \right] e_y, \quad (38a)$$

$$h_z = \left[\frac{k \mu_{xx} + i \gamma_2 \mu_{xz}}{\omega \mu_0 \mu_{xx} \mu_V} \right] e_y. \quad (38b)$$

The nonlinear dispersion relation can now be obtained by applying the electromagnetic usual boundary equations. From the continuity of tangential \mathbf{H} at $z=0$ we get, from Eq. (38a)

$$-\left[\frac{\gamma_2\mu_{xx} + ik\mu_{xz}}{\omega\mu_0\mu_{xx}\mu_V}\right]e_L = h_{x1}(0), \quad (39)$$

where $e_L = -iE_L$. From the continuity of normal \mathbf{B} at $z=0$ we get

$$-\mu_{xz}h_{x2}(0) + i\mu_{xx}h_{z2}(0) = i(\mu_L + \alpha|h_1|^2)h_{z1}(0). \quad (40)$$

The subscripts 2 and 1 in Eqs. (39) and (40) denote the linear and nonlinear media, respectively. Eliminating $h_{x2}(0)$ and $h_{z2}(0)$ from Eq. (40), with the aid of Eqs. (38) yields

$$\left[\frac{\mu_{xz}(\gamma_2\mu_{xx} + ik\mu_{xz})}{\omega\mu_0\mu_{xx}\mu_V} + \frac{i\mu_{xx}(k\mu_{xx} + i\gamma_2\mu_{xz})}{\omega\mu_0\mu_{xx}\mu_V}\right]e_L = i[\mu_L + \alpha h_1^2(0)]h_{z1}(0), \quad (41)$$

which can be simplified to

$$\frac{k}{\omega\mu_0}e_L = [\mu_L + \alpha h_1^2(0)]h_{z1}(0). \quad (42)$$

We can eliminate e_L from Eqs. (39) and (42) and obtain the relation

$$-(\gamma_2\mu_{xx} + ik\mu_{xz})[\mu_L + \alpha(A_0^2 + h_{z1}^2(0))]h_{z1}(0) = k\mu_{xx}\mu_V A_0, \quad (43)$$

where $A_0 = h_{x1}(0)$ can be regarded as a nonlinear parameter.

Equation (43) together with the first integral given by Eq. (35) determines the nonlinear dispersion relation. In order to obtain this explicitly, we must eliminate $h_{z1}(0)$ from these two equations. Although this is difficult to do for a general nonlinearity, it can be done rather simply for the case of weak nonlinearity.

Let us rewrite Eq. (43) as

$$\alpha h_{z1}^3(0) + \alpha A_0^2 h_{z1}(0) + \mu_L h_{z1}(0) + \frac{k\mu_{xx}\mu_V}{\gamma_2\mu_{xx} + ik\mu_{xz}} A_0 = 0, \quad (44)$$

and assume that $\alpha h_{z1}^2(0) \ll \mu_L$, $\alpha A_0^2 \ll \mu_L$. We set

$$h_{z1}(0) = h_{z1}^{(1)} + \Delta, \quad (45)$$

where

$$h_{z1}^{(1)} = -\frac{k\mu_{xx}\mu_V A_0}{\mu_L(\gamma_2\mu_{xx} + ik\mu_{xz})} \quad (46)$$

and Δ is $O(\alpha)$, and substitute into Eq. (44). Neglecting terms of higher order than the first in α , we find that

$$\Delta = -\frac{\alpha h_{z1}^{(1)}}{\mu_L} [(h_{z1}^{(1)})^2 + A_0^2], \quad (47)$$

and hence

$$h_{z1} \simeq h_{z1}^{(1)} \left[1 - \frac{\alpha}{\mu_L} [(h_{z1}^{(1)})^2 + A_0^2] \right]. \quad (48)$$

If we define

$$G = -\frac{k\mu_{xx}\mu_V}{\mu_L(\gamma_2\mu_{xx} + ik\mu_{xz})}, \quad (49)$$

then $h_{z1}^{(1)} = G A_0$, and Eq. (48) becomes

$$h_{z1} \simeq G A_0 \left[1 - \frac{\alpha A_0^2}{\mu_L} (1 + G^2) \right]. \quad (50)$$

Eliminating h_{x1} and h_{z1} from Eq. (35) in favor of A_0 and G yields the nonlinear dispersion relation in the form

$$n^2(G^2 - 1) - \epsilon_1\mu_L G^2 - \frac{\alpha}{2\mu_L}(G^2 + 1) \times [(3G^2 - 1)n^2 - 2\epsilon_1\mu_L G^2] A_0^2 = 0, \quad (51)$$

where we have discarded terms of second order and higher in α . If we let $\alpha \rightarrow 0$, we obtain

$$n^2 = \frac{\epsilon_1\mu_L G^2}{G^2 - 1}, \quad (52)$$

which corresponds to the linear dispersion relation of Hartstein *et al.*

In Eq. (51) the dominant k terms can be determined by letting $k \rightarrow \pm\infty$ to give $G^2 \rightarrow (G^{(\pm)})^2$, where now

$$(G^2 - 1) - \frac{\alpha}{2\mu_L}(G^2 + 1)(3G^2 - 1)A_0^2 = 0, \quad (53)$$

which gives

$$G^2 \simeq \frac{\mu_L}{3\alpha A_0^2} - \frac{1}{3} \pm \left[\frac{\mu_L}{3\alpha A_0^2} - \frac{4}{3} - \frac{6\alpha A_0^2}{\mu_L^2} \dots \right] = 1 + \frac{2\alpha A_0^2}{\mu_L} = 1 + \frac{\Gamma}{\mu_L^2}. \quad (54)$$

where $\Gamma = 2\alpha A_0^2 \mu_L$.

V. ASYMPTOTIC LIMITS FOR LARGE WAVE NUMBER: TE WAVES

As $k \rightarrow \pm\infty$, $\gamma_2 \rightarrow |k|$ and

$$G^{(+)} = -\frac{\mu_{xx}\mu_V}{\mu_1(\mu_{xx} + i\mu_{xz})}, \quad G^{(-)} = \frac{-\mu_{xx}\mu_V}{\mu_1(\mu_{xx} - i\mu_{xz})}, \quad (55)$$

so that the large k limits of the nonlinear dispersion equation are given by

$$(\mu_{xx} - i\mu_{xz})^2 - \mu_1^2 = \Gamma \quad \text{for } k > 0, \quad (56)$$

$$(\mu_{xx} + i\mu_{xz})^2 - \mu_1^2 = \Gamma \quad \text{for } k < 0. \quad (57)$$

If $\Gamma = 0$ and the nonlinearity disappears then these limits yield

$$\mu_{xx} - i\mu_{xz} = \pm\mu_1 \quad \text{for } k > 0, \quad (58)$$

with possible solutions

$$\omega_+ = \omega_0 + \frac{\mu_2}{\mu_2 - \mu_1} \omega_m, \quad (59a)$$

$$\omega_- = \omega_0 + \frac{\mu_2}{\mu_2 + \mu_1} \omega_m. \quad (59b)$$

The original unsquared dispersion relationship is

$$\mu_{xx} - i\mu_{xz} = -\mu_1, \quad (60)$$

however, so that only ω_- is an acceptable solution. For $k < 0$

$$\mu_{xx} + i\mu_{xz} = \pm\mu_1, \quad (61)$$

with possible solutions

$$\omega_+ = -\omega_0 - \frac{\mu_2}{\mu_2 - \mu_1} \omega_m, \quad (62a)$$

$$\omega_- = -\omega_0 - \frac{\mu_2}{\mu_2 + \mu_1} \omega_m. \quad (62b)$$

The original unsquared dispersion equation is

$$\mu_{xx} + i\mu_{xz} = -\mu_1, \quad (63)$$

so that ω_+ must be disregarded. In this case, however, since ω_- is negative no large k limit exists at all.

The inclusion of nonlinearity changes Eqs. (58) and (61) to

$$(\mu_2^2 - \mu_1^2 - \Gamma)\omega^2 + 2[-\mu_2^2(\omega_m + \omega_0) + \omega_0(\mu_1^2 + \Gamma)]\omega + \mu_2^2(\omega_0 + \omega_m)^2 - \omega_0^2(\mu_1^2 + \Gamma) = 0 \quad \text{for } k > 0, \quad (64)$$

$$(\mu_2^2 - \mu_1^2 - \Gamma)\omega^2 + 2[\mu_2^2(\omega_m + \omega_0) - \omega_0(\mu_1^2 + \Gamma)]\omega + \mu_2^2(\omega_0 + \omega_m)^2 - \omega_0^2(\mu_1^2 + \Gamma) = 0 \quad \text{for } k < 0. \quad (65)$$

The possible solutions of these quadratic equations, filtering out the extra solutions that appear through squaring,

are

$$\omega = \omega_0 + \frac{\mu_2^2 \omega_m}{\mu_2^2 - \mu_1^2 - \Gamma} - \frac{\mu_2 \omega_m (\mu_1^2 + \Gamma)^{1/2}}{\mu_2^2 - \mu_1^2 - \Gamma} \quad \text{for } k > 0, \quad (66)$$

$$\omega = - \left[\omega_0 + \frac{\mu_2^2 \omega_m}{\mu_2^2 - \mu_1^2 - \Gamma} \right] + \frac{\mu_2 \omega_m (\mu_1^2 + \Gamma)^{1/2}}{\mu_2^2 - \mu_1^2 - \Gamma} \quad \text{for } k < 0. \quad (67)$$

Several cases can now be developed, taking as an example a self-focusing situation in which $\alpha > 0$ and $\Gamma > 0$. The $k > 0$ cases are

$$\text{case A: } \mu_2 \approx \mu_1 \approx 1, \quad |\mu_2^2 - \mu_1^2| \ll \Gamma, \quad \Gamma \ll 1, \quad (68)$$

$$\omega \approx \omega_0 + \frac{\omega_0}{2} + O(\Gamma),$$

$$\text{case B: } \mu_2 < \mu_1, \quad 0 < \Gamma \leq |\mu_2^2 - \mu_1^2|, \quad (69)$$

$$\omega \approx \omega_0 + \frac{(\mu_2 - \mu_1)\mu_2 \omega_m}{(\mu_2^2 - \mu_1^2) - \Gamma}.$$

It appears that when $\Gamma \approx (\mu_2 - \mu_1)$, the nonlinearity will significantly alter the larger $k > 0$ limit. For $k < 0$ we have

$$\text{case A: } \mu_2 \approx \mu_1 \approx 1, \quad |\mu_2^2 - \mu_1^2| \ll \Gamma, \quad \Gamma \ll 1, \quad (70)$$

$$\omega \approx -\omega_0 + \frac{\omega_m}{2} + O(\Gamma),$$

$$\text{case B: } \mu_2 > \mu_1, \quad |\mu_2^2 - \mu_1^2| \leq \Gamma, \quad (71)$$

$$\omega \approx \omega_m \left[\frac{\mu_2(\mu_2 - \mu_1)}{\Gamma - (\mu_2^2 - \mu_1^2)} - \frac{\omega_0}{\omega_m} \right].$$

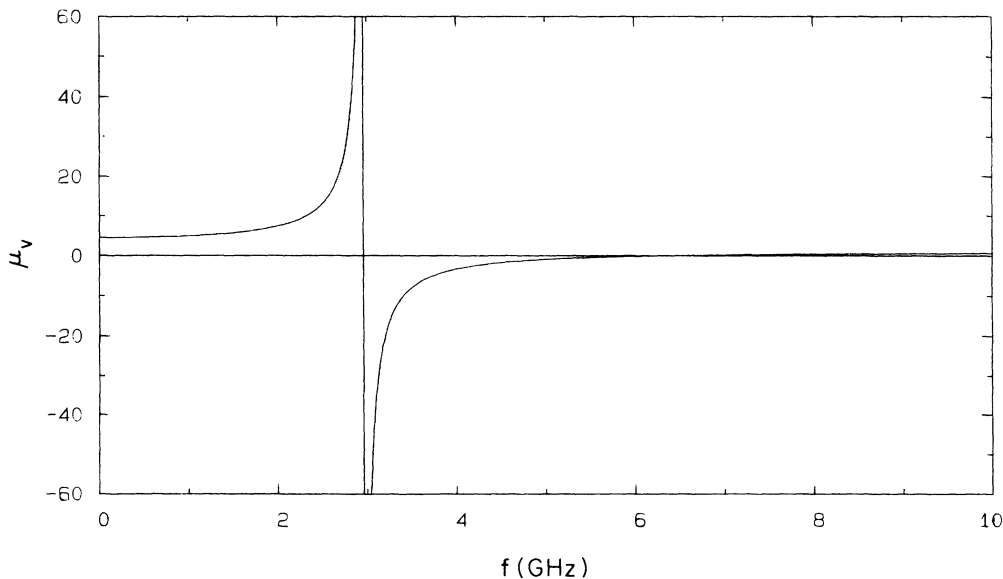


FIG. 6. The effective permeability μ_v as a function of frequency f . $\mu_0 H_0 = 500$ G, $\mu_0 M_0 = 1750$ G, $\gamma = 2\pi(2.8) \times 10^6$ rad s $^{-1}$ G $^{-1}$. $\mu_2 = \mu_B = 1.25$.

Here we see the possibility of propagation induced in the $k < 0$ direction simply by balancing the value of Γ with $\mu_1 - \mu_1$.

VI. TE WAVES POWER FLOW

The power flow P , in the direction of propagation is in this case,

$$P = \frac{1}{2} \int E_y H_z^* dz . \quad (72)$$

P^{NL} power flow in the nonlinear medium is

$$P^{\text{NL}} = \frac{\omega \mu_0}{2k_0} \int_0^\infty \mu^{\text{NL}} |H_z|^2 dz = \frac{\omega \mu_0}{2k} \int_0^\infty \mu^{\text{NL}} h_z^2 dz . \quad (73)$$

P^L , the power flow in the linear medium, is

$$P^L = \frac{\omega \mu_0 \mu_{xx} \mu_V}{2(k \mu_{xx} + i \gamma_2 \mu_{xz})} \int_{-\infty}^0 h_z^2 dz . \quad (74)$$

If h_z is eliminated in favor of h_x by means of Eqs. (38) and the z dependence of h_x in the linear medium is given by

$$h_x(z) = A_0 e^{\gamma_2 z} . \quad (75)$$

Then the result for the power flow in the linear medium is

$$P^L = \frac{\omega \mu_0 \mu_{xx} \mu_V (k \mu_{xx} + i \gamma_2 \mu_{xz}) A_0^2}{4 \gamma_2 (\gamma_2 \mu_{xx} + i k \mu_{xz})^2} . \quad (76)$$

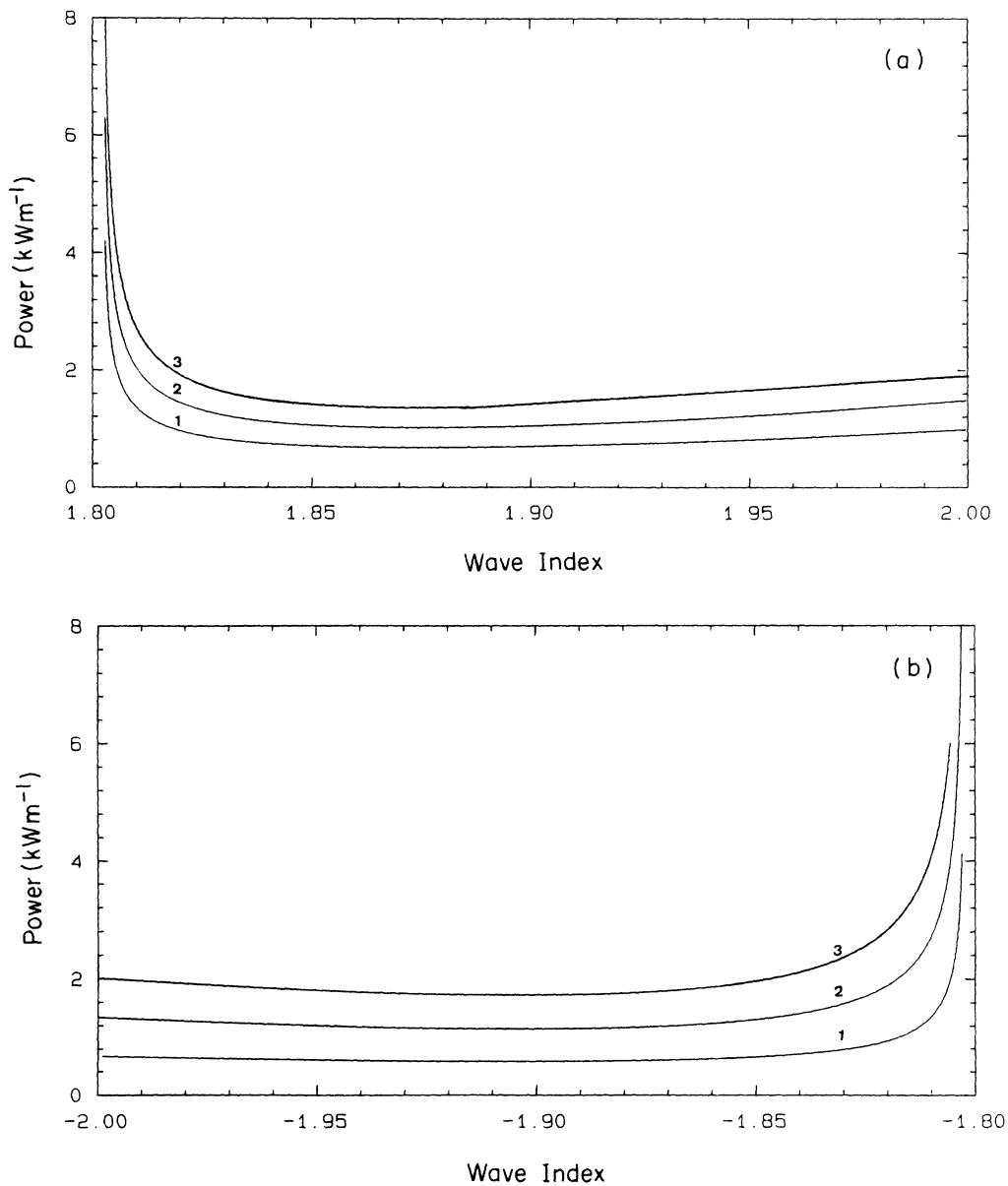


FIG. 7. TE waves $\mu_V > 0$. (a) Power flow as a function of wave index ($k > 0$). (b) Power flow as a function of wave index ($k < 0$). $\mu_0 H_0 = 500$ G, $\mu_0 M_0 = 1000$ G. $\mu_V = 3.24$, $\mu_1 = \mu_L = 1.29$, $\epsilon_1 = \epsilon_L = 2.3$, $\epsilon_2 = 1$. $\alpha = 8.869 \times 10^{-8} \text{ m}^2 \text{ A}^{-2}$. The labels on the curves mean the following: 1, α ; 2, $\alpha/2$; 3, $\alpha/3$. $\mu_2 = \mu_B = 1.25$.

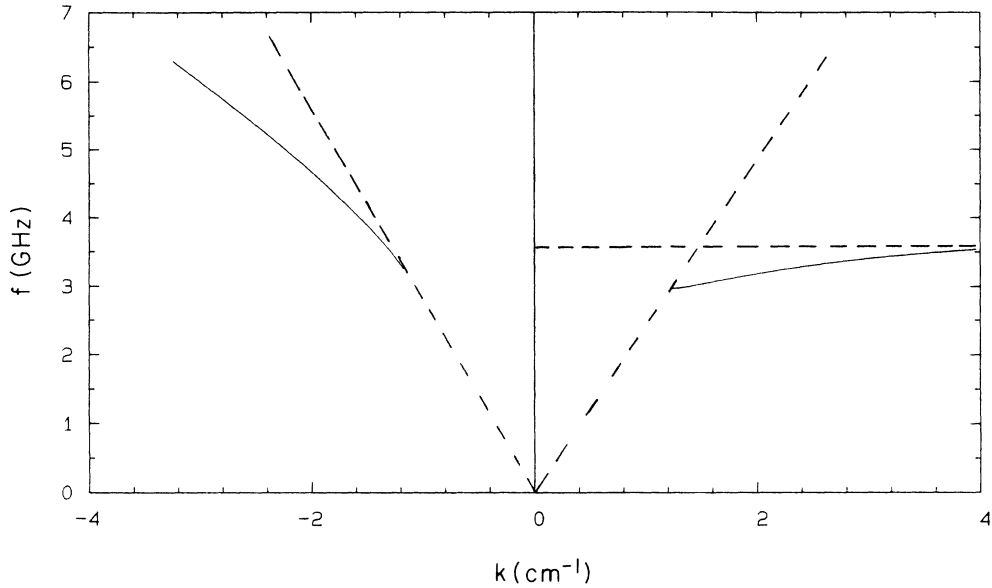


FIG. 8. TE waves $\mu_V < 0$: Typical linear dispersion curves for a vacuum-bounded semi-infinite ferromagnetic substrate when $\mu_V < 0$. The curves exhibit three endpoints and the right-hand branch is asymptotic to the horizontal dashed line.^{18,22} $\mu_0 M_0 = 1750$ G, $\mu_0 H_0 = 500$ G, $\epsilon_2 = 16$, $\mu_2 = 1$.

The exact evaluation of P^{NL} can only be done numerically for $\mu_V < 0$, but, for $\mu_V > 0$, an approximate analytic treatment can be carried out that gives rather good results.⁵ We proceed by using Eq. (29b) to eliminate h_z in favor of e_y in Eq. (73) to give

$$P^{NL} = \frac{k}{2\omega\mu_0} \int_0^\infty \frac{e_y^2}{\mu^{NL}} dz. \quad (77)$$

If it is assumed that $\alpha > 0$, then the electric field com-

ponent e_y reaches its maximum value e_{ym} at the value of z where the integrand is a maximum. We can therefore write to a good approximation that

$$P^{NL} \simeq k \Delta z e_{ym}^2 / \left[2\omega\mu_0 \left(\mu_L + \frac{\alpha k^2}{\omega^2 \mu_0^2 \mu_L^2} - e_{ym}^2 \right) \right], \quad (78)$$

where Δz is a suitable interval about the maximum.⁵

At the maximum of e_y , $\partial e_y / \partial z = 0$ and hence from Eq. (29a) we have $h_x = 0$. If we take the first integral in the

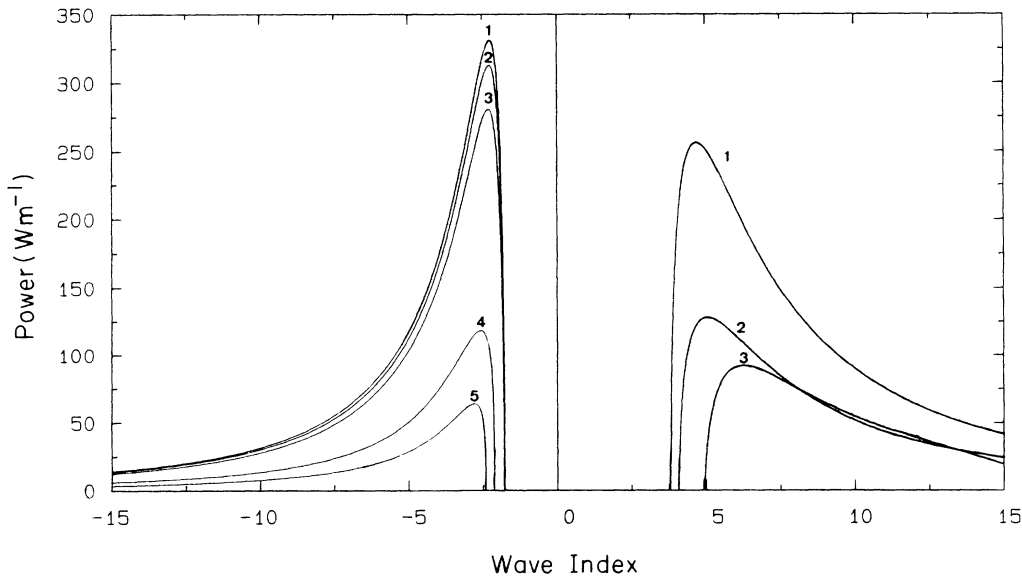


FIG. 9. TE waves $\mu_V < 0$: Power-wave index variation for $\mu_V < 0$. Curves are labeled as follows. 1, $P/10$ — $f = 3.25$ GHz, $\mu_V = -16.72$; 2, $P/10$ — $f = 3.35$ GHz, $\mu_V = -11.85$; 3, $P/10$ ($k < 0$), $P \times 100$ ($k > 0$)— $f = 3.45$ GHz, $\mu_V = -9.01$; 4, $P \times 100$ — $f = 3.50$ GHz, $\mu_V = -8$; 5, $P \times 1000$ — $f = 3.55$ GHz, $\mu_V = -7.16$. $\epsilon_1 = \epsilon_L = 2.3$, $\mu_1 = \mu_L = 1.29$, $\epsilon_2 = 16$, $\alpha = 8.869 \times 10^{-8}$ m² A⁻². $\mu_0 H_0 = 500$ G, $\mu_0 M_0 = 1750$ G. Note that P is the true value of the power.

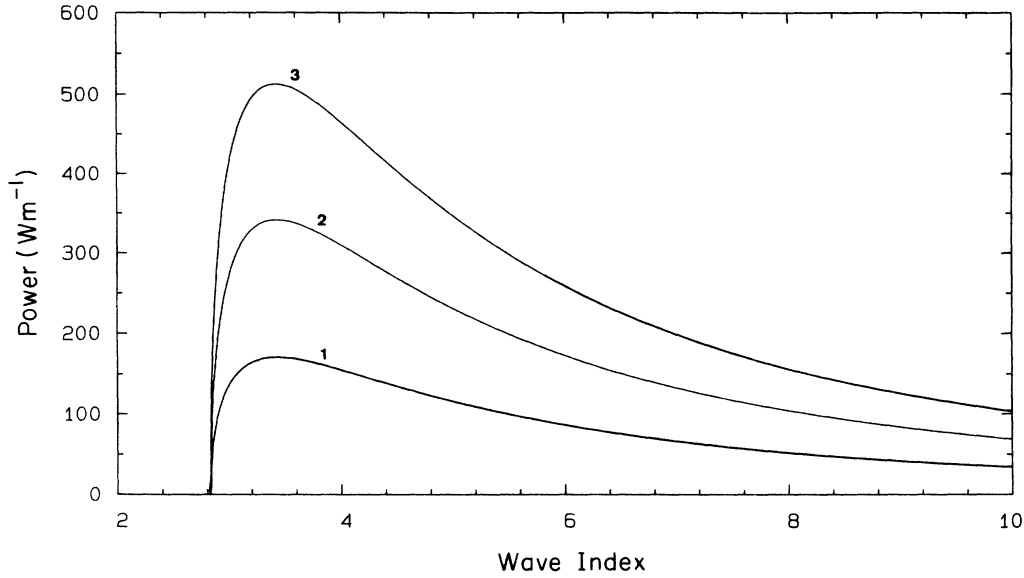


FIG. 10. TE waves $\mu_v < 0$: Power-wave index variation. The curves, in ascending order, correspond to α , $\alpha/2$, and $\alpha/3$. $\epsilon_2 = 16$, $\epsilon_1 = \epsilon_L = 2.3$, $\mu_v = -13.91$, $f = 3.3$ GHz, $\mu_0 M_0 = 1750$ G, $\mu_0 H_0 = 500$ G. $\mu_2 = 1$.

form given by Eq. (34) and carry out some elementary manipulations, we obtain

$$(2k^2 - k_0^2 \epsilon_1 \mu^{\text{NL}}) e_y^2 - \omega^2 \mu_0^2 \mu^{\text{NL}} \left[\mu_L h^2 + \frac{\alpha}{2} h^4 \right] = 0. \quad (79)$$

$$-\frac{k^2}{\mu^{\text{NL}}} \left[\mu_L e_{ym}^2 + \frac{\alpha k^2}{\omega^2 \mu_0^2 (\mu^{\text{NL}})^2} e_{ym}^4 \right] = 0 \quad (81)$$

Setting $h_x = 0$ and making the substitution

$$h_z = \frac{k}{\omega \mu_0 \mu^{\text{NL}}} e_y \quad (80)$$

with

$$\mu^{\text{NL}} = \mu_L + \frac{\alpha k^2}{\omega^2 \mu_0^2 (\mu^{\text{NL}})^2} e_{ym}^2. \quad (82)$$

from Eq. (29b), we can transform Eq. (79) to

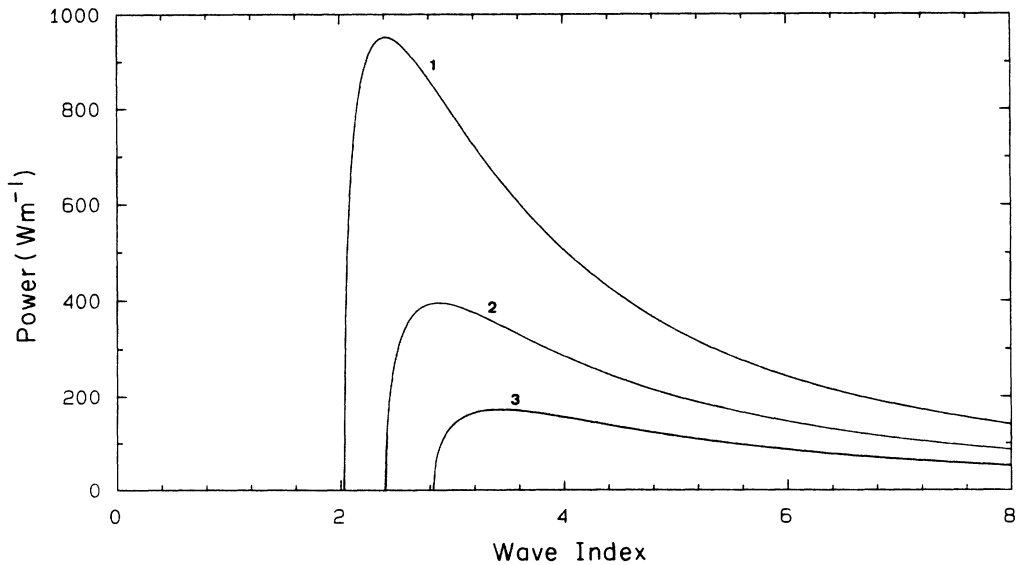


FIG. 11. TE waves $\mu_v < 0$: Power-wave index variation. The curves correspond to the frequencies 2.97 GHz (-4511), 3.0 GHz (-170), 3.05 GHz (-62.98), in ascending order. Values of μ_v are given in parentheses.

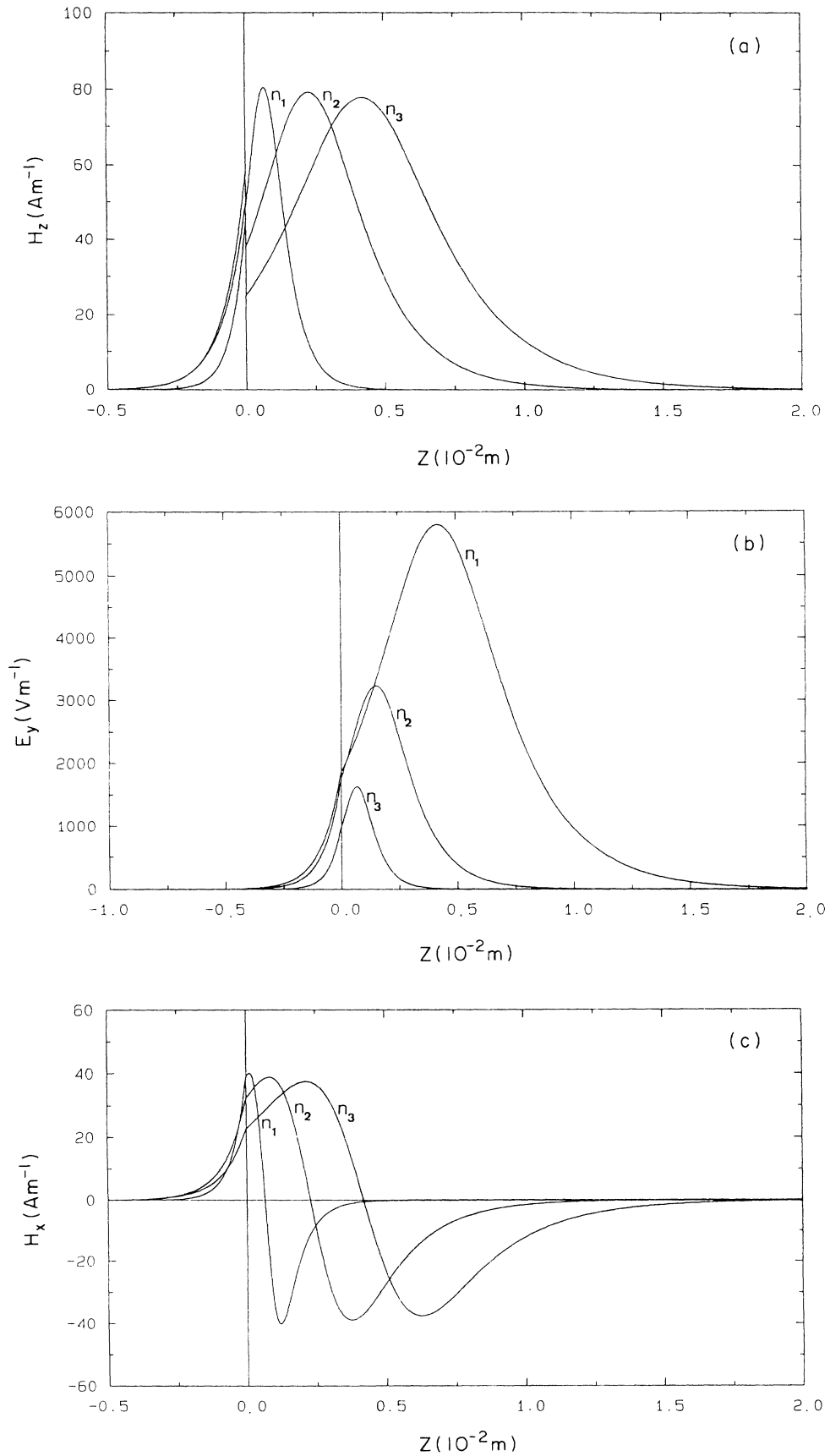


FIG. 12. TE waves $\mu_v < 0$: (a) H_z , (b) E_y , and (c) H_x variation across the interface for four different values of wave index, $n_1=2.62$, $n_2=9$, $n_3=12$, $n_4=18$. $f=3.25$ GHz, $\mu_v=-6.72$, $\alpha=8.869 \times 10^{-8} \text{ m}^2 \text{ A}^{-2}$.

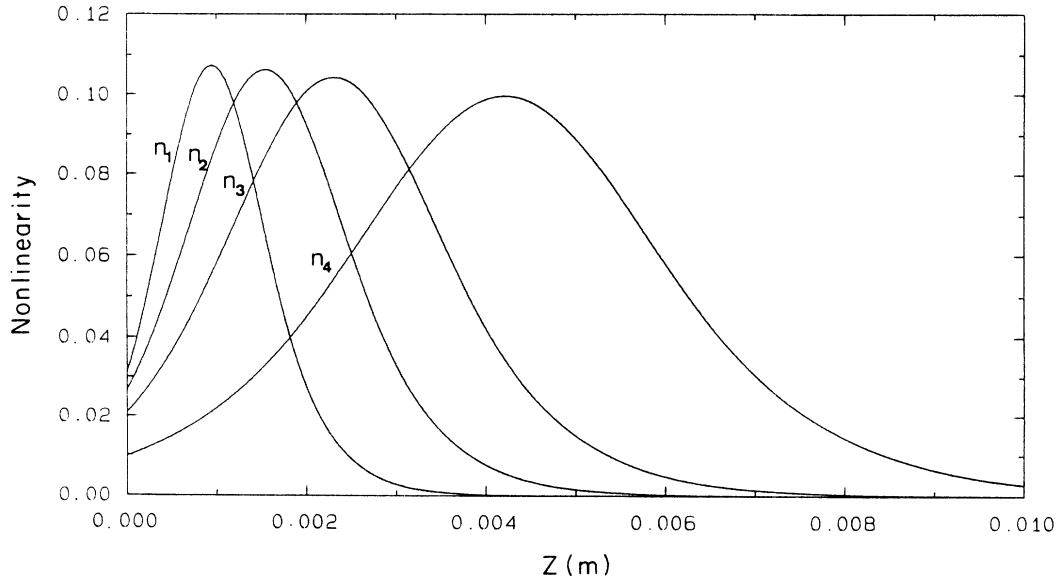


FIG. 13. TE waves $\mu_V < 0$: Nonlinearity as a function of distance from the interface.

VII. NUMERICAL RESULTS FOR TE WAVES

A. $\mu_V > 0$

The parameters used here are listed in Table I and the appropriate μ_V , which is frequency dependent, is given in the figure captions. In the Voigt propagation geometry of Fig. 1, TE waves in the linear limit are controlled by the effective permeability μ_V that is defined as $\mu_{xx} + \mu_{xz}^2/\mu_{xx}$. Linear surface polaritons can propagate provided that $\mu_V < 0$. A dominant feature of nonlinear wave propagation, as has already been shown for TM waves, is the possibility of wave propagation in regimes for which there is no linear limit. Accordingly, the frequency region to the left of the resonance in Fig. 6, for which $\mu_V > 0$, is also of interest here and will allow nonlinear waves to be sustained above a threshold power. Since TE waves are associated with both H_x and H_z magnetic field components they will depend upon the frequency-dependent μ_{xx} and μ_{xy} components of the permeability tensor as expressed through μ_V .

The power curves shown in Fig. 7 show a power threshold but the curves now approach infinity both at a lower cutoff $n = \sqrt{\mu_V}$ and as $n \rightarrow \infty$. The peak of the self-focused field moves out to infinity for both TE and TM modes but the distinction between the two modes is that n has no bound for TE waves, i.e., as the self-focused field moves out to infinity, $n \rightarrow \infty$. One of the features to be looked for here is whether the nonreciprocal behavior, often associated with magnetic materials, is present. As can be seen in Fig. 7, this is not very strong here, with only a slight asymmetry being detectable.

B. $\mu_V < 0$

$\mu_V < 0$ in a frequency range to the right of the singularity in Fig. 6. For these frequencies the interface can sup-

port linear TE surface waves. For $\mu_0 H_0 = 500$ G and $\mu_0 M_0 = 1750$ G, the resonance frequency is $f_r = 3$ GHz. The linear dispersion curves shown in Fig. 8 are well known, in principle, but have been recalculated here for ease of reference. They possess several main points of interest. These are (1) defined end or cutoff points, (2) propagation characteristics to the left ($k < 0$) and to the right ($k > 0$) that are not symmetrical, and (3) only the right-hand-propagation dispersion curve having a large wave-number limit and this tending to the familiar magnetostatic limit.

For a sequence of frequencies, labeled (1)–(5), that cause μ_V to line in the range $-7.16 \leq \mu_V \leq -16.72$ the variation of the wave index with total power flow is given in Fig. 9. The curves labeled (1), (2), and (3) lie on both the $k > 0$ and $k < 0$ branches of Fig. 8, while (4) and (5) lie only on the $k < 0$ branch. The expected nonreciprocal behavior shows a strong dependence upon power. For a given frequency, the power flow can be significantly greater in one direction than in the other. This could lead to some interesting experimental possibilities involving nonreciprocal nonlinear power transfer. Figure 10 and 11 show, on an expanded scale, the $k > 0$ power curves as the nonlinear coefficient α or ω (μ_V) is varied. Since the nonlinearity is weakened by diminishing α or ω , higher peak values must be reached in both cases to enter the strongly nonlinear regimes.

The variation of the H_x, H_z, E_y , field components is shown in the sequence Figs. 12(a), 12(b), and 12(c) with the nonlinear medium on the right-hand side. Several values of frequency are selected corresponding to different positions on the (μ_V, f) curve.

As a final numerical example, Fig. 13 shows the nonlinearity, defined as $\alpha|\mathbf{H}|^2$, as a function of z measured from the interface for $\mu_V = -6.716$ and several values of n . The nonlinearity increases in strength as n increases.

The absolute values of the nonlinearity appear to be within the reach of experimental observation.

VIII. CONCLUSIONS

The theory of nonlinear TM and TE wave propagating along the interface between two semi-infinite magnetic media has been presented. Exact solutions are given for a certain type of nonlinear magnetic medium that could be created artificially.¹⁶ Since there has been recent experimental progress on artificial enhanced nonlinear nonmagnetic dielectric media¹² at microwave frequencies, there is every reason to expect the magnetic systems, also with an enhanced nonlinearity, consisting of suspensions of microspheres, can be created.¹⁶ The calculations reported here, therefore, represent a starting point for a new area of work in magnetodynamic and magnetostatic wave propagation.

The power levels required for nonlinear magnetic TM waves, since they are in the MW/m range, are of course rather high, and it remains to be seen whether they can be achieved. For nonlinear TE waves we have $\mu_V < 0$ so that the situation is rather different. Since μ_V can be readily adjusted with frequency for the ferromagnetic substrate, we are actually presenting the first calculations in which the required power levels to observe strong non-

linearity can be tuned. Hence, provided that suitably high α material can be found, it is a relatively easy matter to adjust μ_V to reduce the power levels needed to observe strongly nonlinear waves.

In the parallel activity in nonlinear optics the variation of the mode index with power is often regarded as implying the possibility of optical switching. Roughly speaking this is because a *single* power level can be given by more than one wave index. Furthermore, it is a general rule that the negative slopes of the power curves are quite likely to be unstable. Hence in an experiment, involving the variation of the input power into a surface-guided wave with its output power,^{1,7} bistability, hysteresis, or some form of switching⁷ can be expected. The single interface calculation reported here represents only a beginning for the theoretical foundations, since a thin-film format, involving a periodic structure, is likely to be more attractive experimentally. It is hoped, however, this paper will act as a stimulus for further work in this area.

ACKNOWLEDGMENTS

A.D.B. and R.W. wish to thank NATO for support from collaborative Grant No. RG.86/0474 on "Non-linear Electromagnetic Guided Waves on Magneto-optic and Magnetic Structures."

-
- ¹A. D. Boardman and P. Egan, *IEEE J. Quantum Electron.* **QE-21**, 1701 (1985).
²D. Mihalache, D. Mazilu, and F. Lederer, *Opt. Commun.* **B 59**, 107 (1986).
³A. D. Boardman, A. A. Maradudin, G. I. Stegeman, T. Twardowski, and E. M. Wright, *Phys. Rev. A* **35**, 1159 (1987).
⁴A. D. Boardman and T. Twardowski, *Phys. Rev. A* **39**, 2481 (1989).
⁵A. D. Boardman, T. Twardowski, A. Shivarova, and G. I. Stegeman, *IEE Proc. J.* **134**, 152 (1987).
⁶G. I. Stegeman and C. T. Seaton, *Opt. Lett.* **9**, 235 (1984).
⁷C. T. Seaton, J. D. Valera, R. L. Shoemaker, G. I. Stegeman, J. T. Chilwell, and S. D. Smith, *IEEE J. Quantum Electron.* **QE-21**, 774 (1985).
⁸T. P. Shen, G. I. Stegeman, and A. A. Maradudin, *J. Opt. Soc. Am.* **B 5**, 1391 (1988).
⁹J. Zyss, *J. Mol. Electron.* **1**, 25 (1985).
¹⁰P. W. Smith, A. Ashkin, and M. J. Tomlinson, *Opt. Lett.* **6**, 284 (1981).
¹¹P. W. Smith, P. J. Maloney, and A. Ashkin, *Opt. Lett.* **7**, 347 (1982).
¹²B. Bobbs, R. Shih, and H. R. Fetterman, *Appl. Phys. Lett.* **52**, 4 (1988).
¹³C. B. Galanti and C. L. Giles, *SPIE* **517**, 219 (1984).
¹⁴A. D. Boardman and S. A. Nikitov, *Phys. Rev. B* (to be published).
¹⁵A. K. Zvezdin and A. F. Popkov, *Zh. Eksp. Teor. Fiz.* **84**, 606 (1983) [*Sov. Phys.—JETP* **57**, 350 (1983)].
¹⁶M. Bertolotti, C. Sibilila, and I. Fuli, *Int. Infrared Millimeter Waves* **8**, 723 (1987).
¹⁷A. J. Palmer, *Opt. Lett.* **5**, 54 (1980).
¹⁸A. D. Boardman, in *Electromagnetic Surface Modes*, edited by A. D. Boardman (Wiley, New York, 1982).
¹⁹A. Hartstein, E. Burstein, A. A. Maradudin, R. Brewer, and R. F. Wallis *et al.*, *J. Phys. C* **6**, 1266 (1973).
²⁰A. D. Karsano and D. R. Tilley, *J. Phys. C* **11**, 3487 (1978).
²¹J. P. Parekh and S. R. Ponamgi, *J. Appl. Phys.* **44**, 1384 (1973).
²²T. J. Gerson and J. S. Nadan, *IEEE Trans. Microwave Theory Tech* **MTT-22**, 757 (1974).
²³J. P. Parekh, *J. Appl. Phys.* **46**, 5040 (1975).
²⁴M. Fukui, H. Dohi, J. Matsuura, and O. Tada, *J. Phys. C* **17**, 1783 (1984).
²⁵N. Marcuvitz, *Waveguide Handbook* (McGraw-Hill, New York, 1951).
²⁶C. Thibaudeau and A. Caillé, *Phys. Rev. B* **32**, 5911 (1985).